Journal of Power Sources 185 (2008) 1429–1433

Contents lists available at ScienceDirect

Journal of Power Sources

journal homepage: www.elsevier.com/locate/jpowsour

Short communication

Influence of Co substitution for Ni and Mn on the structural and electrochemical characteristics of $LiNi_{0.5}Mn_{1.5}O_4$

Atsushi Ito [a], Decheng Li [b], Yunsung Lee [c], Koichi Kobayakawa [a], Yuichi Sato [a,*]

[a] Department of Applied Chemistry, Faculty of Engineering, Kanagawa University, 3-27-1 Rokkakubashi, Kanagawa-ku, Yokohama 221-8686, Japan
[b] High-Tech Research Center, Kanagawa University, 1-1-40 Suehiromachi, Tsurumi-ku, Yokohama 230-0045, Japan
[c] Faculty of Applied Chemical Engineering, Chonnam National University, 300 Yongbong Dong, Kwangju 500-757, Republic of Korea

ARTICLE INFO

Article history:
Received 19 August 2008
Received in revised form 28 August 2008
Accepted 28 August 2008
Available online 7 September 2008

Keywords:
Li-ion battery
Cathode material
$LiNi_{0.5-x}Co_{2x}Mn_{1.5-x}O_4$
Lithium chemical diffusion coefficient
Area specific impedance
Structural and electrochemical properties

ABSTRACT

$LiNi_{0.5-x}Co_{2x}Mn_{1.5-x}O_4$ ($0 \le 2x \le 0.2$) was prepared by spray drying, then re-annealing in O_2. Their structural and electrochemical properties were studied by ex-situ XRD, GITT, and charge–discharge testing. The substitution of cobalt for Ni and Mn in the $LiNi_{0.5}Mn_{1.5}O_4$ resulted in significant structural and electrochemical variations, such as the change in structural transformation with lithium extraction, the increase in the lithium diffusion coefficient and the decrease in the area specific impedance. Moreover, the improved kinetic properties caused by the Co substitution for Ni and Mn result in an improved cyclic performance at a high rate and at elevated temperature as well as the rate capability.

1. Introduction

$LiNi_{0.5}Mn_{1.5}O_4$ has been extensively studied as a high-voltage cathode material for lithium ion batteries during the past decade, although it was initially proposed as a 3 V cathode material [1–12]. $LiNi_{0.5}Mn_{1.5}O_4$ has a cubic structure, and the valences of Ni and Mn have been determined to be divalent and tetravalent, respectively. When it is charged in the 5 V voltage region, the Ni^{2+} is oxidized to Ni^{4+} via Ni^{3+} during the lithium ion extraction from the lattice, while the valence of Mn does not change [7]. Many efforts have been devoted to the preparation of $LiNi_{0.5}Mn_{1.5}O_4$ through a solution process, such as the sol–gel [2,13], co-precipitation [6,9], emulsion drying [10], molten salt methods [14] and spray dry–post-annealing in O_2 [15], due to the difficulty in the preparation by the traditional solid state reaction [2]. It was found that the cation distribution in the lattice was sensitive to the preparation conditions. $LiNi_{0.5}Mn_{1.5}O_4$, prepared at a high annealing temperature ($\geq$850 °C), adopts a cubic spinel structure with a high symmetry (space group $Fd\dot{3}m$), whereas it adopts a primitive simple cubic structure with a low symmetry (space group $P4_332$) if annealed at a low temperature ($\leq$700 °C) [15]. Moreover, different phase transformation processes occur during the lithium extraction/insertion from/into the lattice, thereby resulting in a different electrochemical behavior [14–17]. In addition to the preparation conditions, the structural and electrochemical properties of the $LiNi_{0.5}Mn_{1.5}O_4$ could also be affected by the substitution of other metal ions, such as Al, Mg, Fe, Cu and Co, and the change in the structural and electrochemical characteristics depends on the dopant [18–22].

Our group previously reported the preparation of $LiNi_{0.5-x}Co_{2x}Mn_{1.5-x}O_4$ ($0 \le 2x \le 0.2$) using a spray dry and post-annealing process, and investigated the influence of the post-annealing process on their structural and electrochemical properties [23]. Although we also found that the substitution of Co for Ni and Mn could result in complicated structural and electrochemical variations, such as the change in the space group, an increase in the oxygen deficiency and cation mixing, and an improved rate capability and cyclic performance, much work is needed to elucidate the influence of Co substitution for Ni and Mn.

In this study, we prepared the $LiNi_{0.5-x}Co_{2x}Mn_{1.5-x}O_4$ ($0 \le 2x \le 0.2$) and investigated its structural and electrochemical variations after the Co substitution.

2. Experimental

The $LiNi_{0.5-x}Co_{2x}Mn_{1.5-x}O_4$ was prepared by a spray dry and post-annealing process. Their preparation method has been

* Corresponding author. Tel.: +81 45 481 5661x3885; fax: +81 45 413 9770.
E-mail address: satouy01@kanagawa-u.ac.jp (Y. Sato).

0378-7753/$ – see front matter © 2008 Elsevier B.V. All rights reserved.
doi:10.1016/j.jpowsour.2008.08.087

reported in Ref. [23]. Generally, the stoichiometric Ni $(NO_3)_2{\cdot}6H_2O$, Co $(NO_3)_2{\cdot}6H_2O$ and Mn $(CH_3COO)_2{\cdot}4H_2O$ were initially dissolved into a 0.2 M citric solution (Ni:Mn:citric acid is 1:3:4 molar ratio.). The resulting solution was pumped into a spray dry instrument (Büchi Mini Spray Dryer B-290). The obtained precursor was pre-heated at 900 °C for 20 h in air. $LiOH{\cdot}H_2O$ was added to the resulting powder (7% molar ratio of lithium is in excess in order to compensate for the possible loss), and the mixture was thoroughly ground, and then pressed into pellets. The pellets were sintered at 700 °C for 24 h in air, and re-treated at 500 °C for 30 h in O_2.

The XRD measurements were carried out using a Rigaku Rint1000 diffractometer equipped with a monochromator and a Cu target tube.

The charge/discharge tests were carried out using a CR2032 coin-type cell, which consisted of a cathode and lithium metal anode separated by a Celgard 2400 porous polypropylene film. The cathode contains a mixture of 20 mg of accurately weighed active materials and 12 mg of teflonized acetylene black (TAB-2) as the conducting binder. The mixture was pressed onto a stainless steel mesh and dried at 130 °C for 4 h. The cells were assembled in a glove box filled with dried argon gas. The electrolyte was 1 M $LiPF_6$ in ethylene carbonate/dimethyl carbonate (EC/DMC, 1:2 by volume).

The Li^+ chemical diffusion coefficients of $LiNi_{0.5-x}Co_{2x}Mn_{1.5-x}O_4$ were measured using the Galvanostatic Intermittent Titration Technique (GITT) by the Nagano BTS2004W charge–discharge system.

3. Results and discussion

Fig. 1 shows the XRD patterns of the $LiNi_{0.5-x}Co_{2x}Mn_{1.5-x}O_4$ $(0 \le 2x \le 0.2)$ prepared by the spray dry process with post-annealing in O_2. All samples had the typical diffraction patterns of a cubic spinel and no impurities were observed in any of the samples.

The initial charge curves of the $LiNi_{0.5-x}Co_{2x}Mn_{1.5-x}O_4$ $(0 \le 2x \le 0.2)$ are shown in Fig. 2. The cells were operated at a current density of 0.2 mA cm^{-2} (20 mA g^{-1}) in the voltage range of 3–4.9 V. A closer inspection revealed that $LiNi_{0.5}Mn_{1.5}O_4$ has two plateaus in its charge profile. One is at about 4.76 V and the other at about 4.77 V. The difference is only 0.01 V. In the case of the $LiNi_{0.475}Co_{0.05}Mn_{1.475}O_4$, the potential of the former decreased to 4.73 V while the latter remained intact. The potential difference between them increased to 0.04 V, and the curve evolved into a significant two-step style. With the increase in the cobalt content, the potential differences between these two plateaus dramatically increase to 0.07, 0.1, and 0.11 V for $2x = 0.1$, 0.15, and 0.2. These results

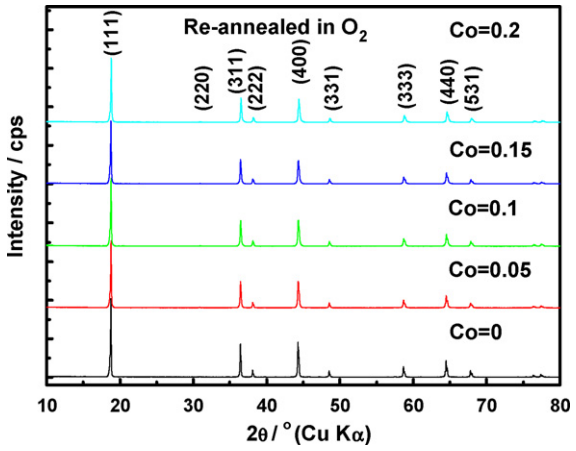

Fig. 1. XRD patterns of the $LiNi_{0.5-x}Co_{2x}Mn_{1.5-x}O_4$ $(0 \le 2x \le 0.2)$ prepared by spray dry process with post-annealing in O_2.

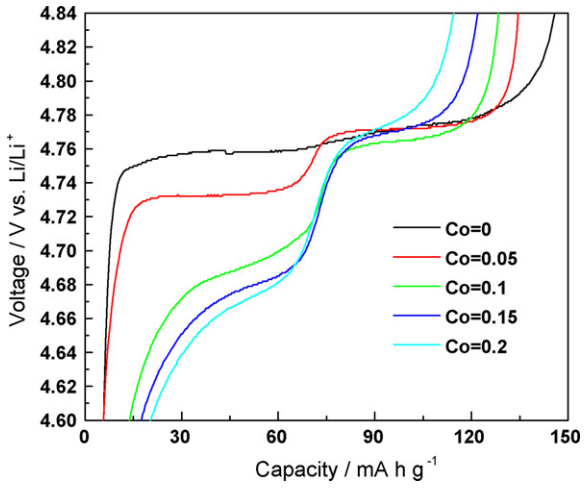

Fig. 2. Initial charge curves of the $LiNi_{0.5-x}Co_{2x}Mn_{1.5-x}O_4$ $(0 \le 2x \le 0.2)$.

implied that the structural evolution behavior of the $LiNi_{0.5}Mn_{1.5}O_4$ with Li-ion extraction from the lattice was affected by the Co substitution of Ni and Mn.

In order to track the structural variation due to lithium extraction from the lattice, the ex-situ XRD measurements of the $LiNi_{0.475}Co_{0.05}Mn_{1.475}O_4$ and $LiNi_{0.45}Co_{0.1}Mn_{1.45}O_4$ were carried out, and their patterns as well as their lattice parameters are shown in Figs. 3 and 4, respectively. Two types of phase transformation behaviors were observed in the $LiNi_{0.475}Co_{0.05}Mn_{1.475}O_4$ and $LiNi_{0.45}Co_{0.1}Mn_{1.45}O_4$ during the lithium extraction process. For the $LiNi_{0.475}Co_{0.05}Mn_{1.475}O_4$, a new phase, which could be denoted as Cubic II (marked with (*)), appears when the cell was charged to 45 mA h g^{-1}. With further charging to 80 mA h g^{-1}, Cubic III (marked with (o)) peaks could be observed, as illustrated in Fig. 3. The first two-phase coexisting region observed in the capacity range from 40 to 75 mA h g^{-1}, consisting of Cubic I and Cubic II, had lattice parameters of 8.168 and 8.081 Å. The second two-phase coexisting region observed in the capacity range from 40 to 75 mA h g^{-1}, consisted of Cubic II and Cubic III and the lattice parameters of Cubic III was 8.010 Å. Moreover, the lattice parameters of the two phases made only a slight adjustment for both two-phase coexisting regions with lithium extraction.

However, in the case of the $LiNi_{0.45}Co_{0.1}Mn_{1.45}O_4$, no new diffraction peaks were observed during the entire charge process, therefore, no obvious two-phase co-existing region was observed in their XRD profiles as depicted in Fig. 4. Moreover, the lattice parameter gradually decreased with the lithium de-intercalation. These results are similar to that of $LiNi_{0.5}Mn_{1.5}O_4$ with different space groups [14], thus we believed that the structural properties of the $LiNi_{0.45}Co_{0.1}Mn_{1.45}O_4$ are intrinsically different from that of the $LiNi_{0.475}Co_{0.05}Mn_{1.475}O_4$, although they have almost the same XRD patterns. As a matter of fact, we have ascribed the space group of $LiNi_{0.45}Co_{0.1}Mn_{1.45}O_4$ to $Fd\bar{3}m$ while $LiNi_{0.475}Co_{0.05}Mn_{1.475}O_4$ should be $P4_332$ based on their different FT-IR spectra from our previous study [23].

Fig. 5 shows the relative lattice volume variation of the $LiNi_{0.5-x}Co_{2x}Mn_{1.5-x}O_4$ after being charged to 4.9 V. The lattice volume of all samples shrinks with the lithium extraction, and the relative volume change gradually decreases from 7% for the $LiNi_{0.5}Mn_{1.5}O_4$ to 4.8% for the $LiNi_{0.4}Co_{0.2}Mn_{1.4}O_4$ as the cobalt content increases. These results suggest that substitution of Co for both Ni and Mn could reduce the relative volume variation, consequently, reduce the risk of the granules exfoliation caused by lithium extraction and enhance the structural stability.

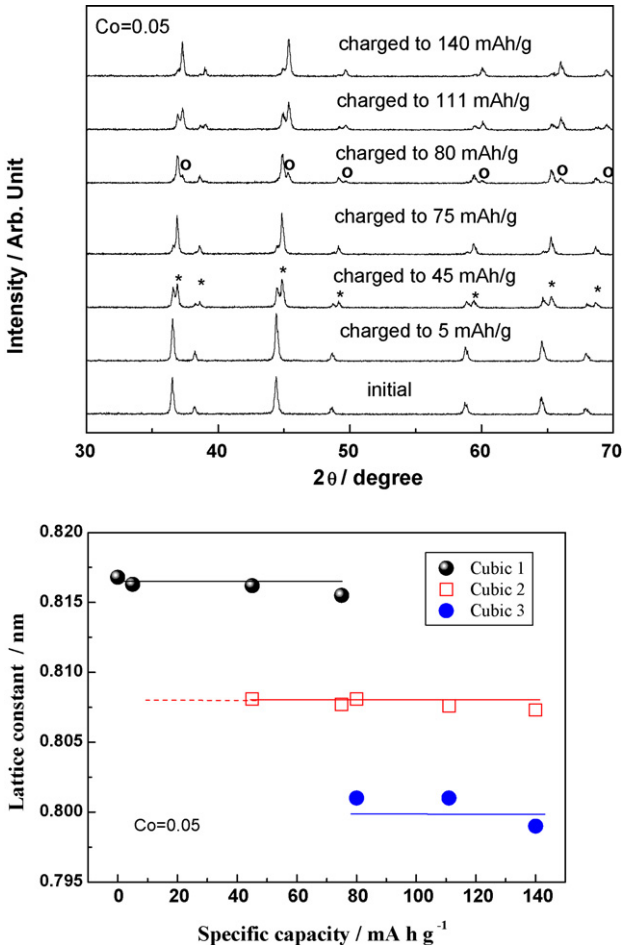

Fig. 3. Ex-situ XRD patterns and lattice parameters of the $LiNi_{0.475}Co_{0.05}Mn_{1.475}O_4$ at different charge states.

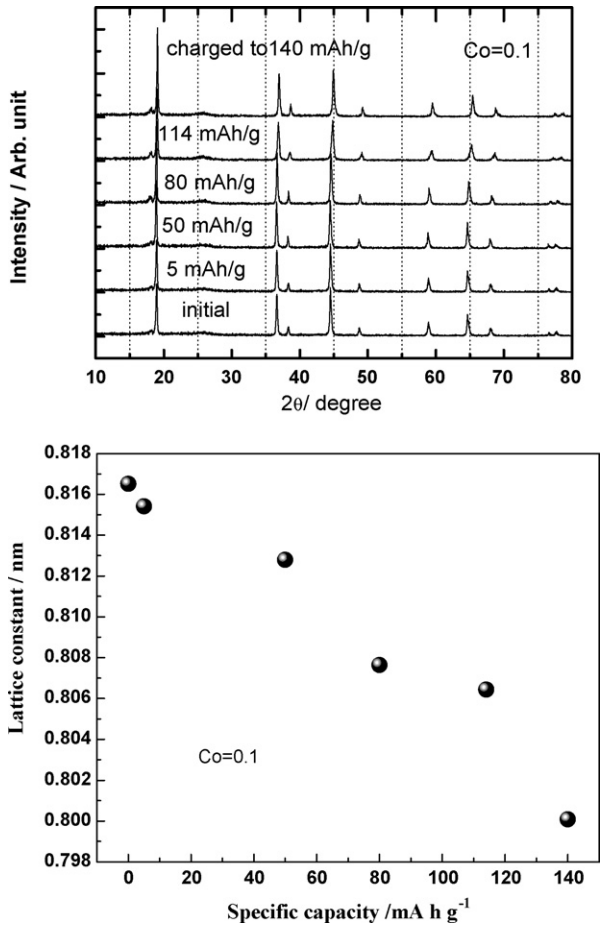

Fig. 4. Ex-situ XRD patterns and lattice parameters of the $LiNi_{45}Co_{0.1}Mn_{1.45}O_4$ at different charge states.

The rate capabilities of the $LiNi_{0.5-x}Co_{2x}Mn_{1.5-x}O_4$ ($0 \le 2x \le 0.2$) with the re-treatment in O_2 are depicted in Fig. 6. All cells were initially operated for one cycle at a current density of 0.2 mA cm^{-2} (20 mA g^{-1}). From the second cycle on, the charge current density was maintained at a constant current density of 0.2 mA cm^{-2}, while the discharge capacities changed from 0.2 mA cm^{-2} (about 0.15 C) to 0.4, 0.8, 1.6, 3.2, and 4.8 mA cm^{-2} (about 3.5 C) in subsequent cycles. The discharge capacity of the $LiNi_{0.5}Mn_{1.5}O_4$ is about 136 mA h g^{-1} at 0.15 C and decreased to about 125 mA h g^{-1} (about 92% of its initial discharge capacity) when the discharge rate increased to 3.5 C. The discharge capacities of the $LiNi_{0.475}Co_{0.05}Mn_{1.475}O_4$ at 0.15 and 3.5 C are 133 and 119 mA h g^{-1}, respectively. Its capacity retention is about 89%, lower than that of the $LiNi_{0.5}Mn_{1.5}O_4$, which should be related to the increased cation mixing degree [23]. The discharge capacities for the samples with $2x = 0.1$, 0.15 and 0.2 are 128, 123, and 116 mA h g^{-1} at 0.15 and 118, 114, and 107 mA h g^{-1} at 3.5 C, respectively. The capacity retention is greater than 92% for all of them. In order to clarify the origin of the improved rate capability, the lithium chemical diffusion coefficients and the area specific impedance (ASI) of the $LiNi_{0.5-x}Co_{2x}Mn_{1.5-x}O_4$ during lithium extraction were determined, and the results are illustrated in Figs. 7 and 8.

Fig. 7 shows the variation in the lithium chemical diffusion coefficients with y in $Li_yNi_{0.5-x}Co_{2x}Mn_{1.5-x}O_4$. The lithium chemical diffusion coefficients of the samples were determined by equation (1).

$$D_{Li^+} = \frac{4}{\pi}\left(\frac{V_m}{nFA}\right)^2\left[I^0\frac{dE/dx}{dE/dt^{1/2}}\right]^2 \quad \text{for } t \ll \left(\frac{(d/2\pi)^2}{D_{Li^+}}\right) \tag{1}$$

where V_m is the molar volume, F is the Faraday constant, A is the contact area between the electrolyte and sample, I^0 is the applied constant electric current, dE/dx is the slope of the coulometric titration curve while $dE/dt^{1/2}$ is the slope of the short-time tran-

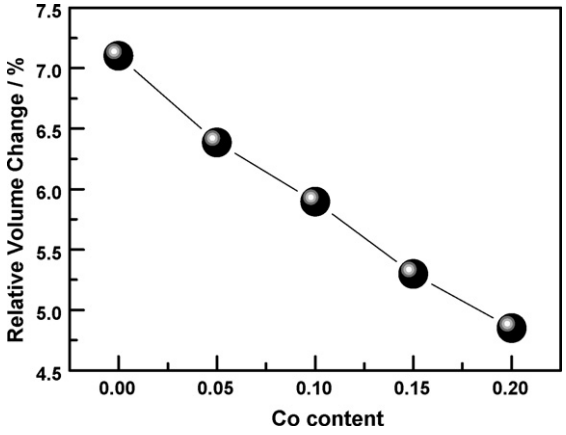

Fig. 5. Relative lattice volume change in the $LiNi_{0.5-x}Co_{2x}Mn_{1.5-x}O_4$ ($0 \le 2x \le 0.2$) after charging to 4.9 V.

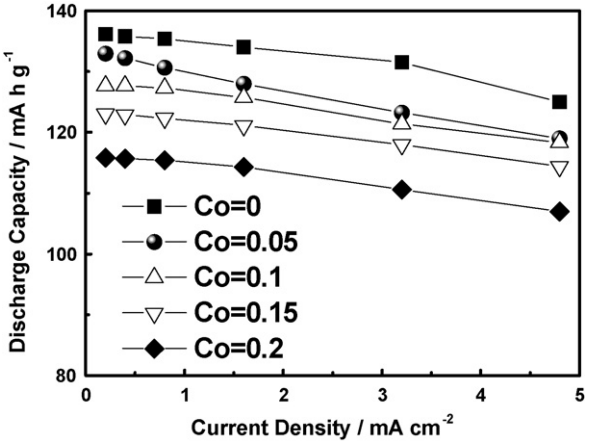

Fig. 6. Rate capabilities of the $LiNi_{0.5-x}Co_{2x}Mn_{1.5-x}O_4$ ($0 \le 2x \le 0.2$).

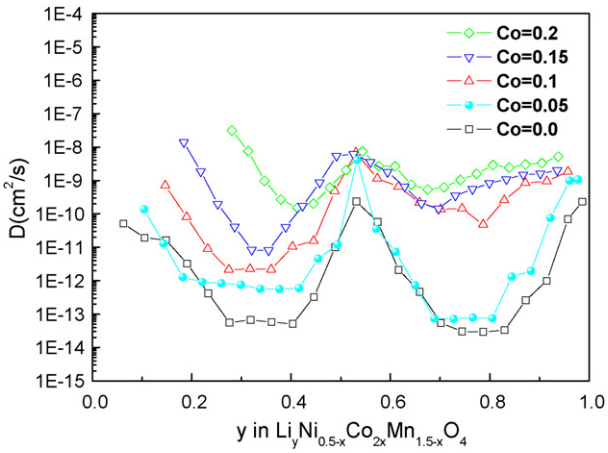

Fig. 7. Li chemical diffusion coefficients vs. Li content in the $LiNi_{0.5-x}Co_{2x}Mn_{1.5-x}O_4$ ($0 \le 2x \le 0.2$).

sient voltage charge. The equation is valid for times shorter than the diffusion time, $(d/2\pi)^2/D_{Li^+}$ where d is the average diameter of the grains [24]. The lithium chemical diffusion of all samples periodically varied with the lithium content in $LiNi_{0.5-x}Co_{2x}Mn_{1.5-x}O_4$. However, the evolution trend of the $LiNi_{0.5}Mn_{1.5}O_4$ and $LiNi_{0.475}Co_{0.05}Mn_{1.475}O_4$ are different from those of the samples with $2x \ge 0.1$. Moreover, the diffusion coefficients remained constant in the range of $0.8 \le y \le 0.7$ and $0.4 \le y \le 0.25$ for these two samples. Since these two regions are consistent well with those of two two-phase coexisting regions in their XRD patterns, we inferred that the lithium diffusion coefficients should be proportional to the velocity of the phase boundary moving. In the case of the samples with $2x \ge 0.1$, the constant diffusion coefficients could not be observed, which should be related to the absence of the two-phase coexisting region for the sample with space group $Fd\dot{3}m$. On the other hand, the diffusion coefficients of the sample with $2x \ge 0.1$ are orders of magnitude higher than that of sample with space group $P4_332$ at every charge state. These results suggest that Co doping could improve the lithium diffusion in the lattice.

Fig. 8 shows the variation in the area specific impedances of the $LiNi_{0.5-x}Co_{2x}Mn_{1.5-x}O_4$ for different state-of-charges (SOC). The voltage variations were measured during the current interruption for 60 s at each SOC for the current 0.4 mA. Similar to that of the lithium diffusion coefficients, the ASI of all samples changed with the lithium extraction from the lattice. However, for almost every charge state, the sample with Co doping exhibits an ASI lower than that of the $LiNi_{0.5}Mn_{1.5}O_4$. These results together with the lithium diffusion data suggest that Co substitution of both Ni and Mn could significantly improve the kinetic properties of the $LiNi_{0.5}Mn_{1.5}O_4$, therefore, improve the rate capability.

Fig. 9 shows the cyclic performances of the $LiNi_{0.5-x}Co_{2x}Mn_{1.5-x}O_4$ ($0 \le 2x \le 0.2$) operated at different C rates in the voltage range of 3–4.9 V at 60 °C. When cells were cycled at 0.15 C, the reversible capacities of the $LiNi_{0.5-x}Co_{2x}Mn_{1.5-x}O_4$

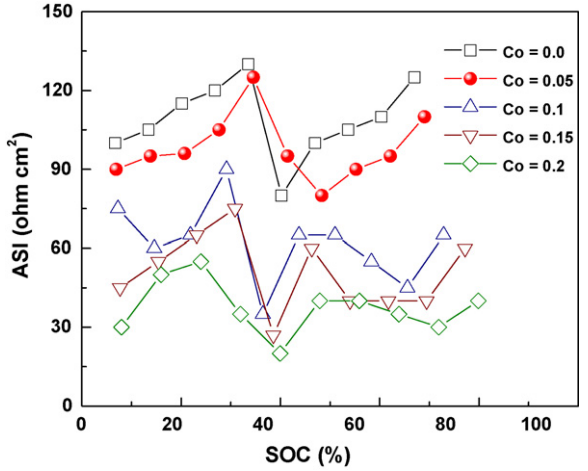

Fig. 8. Area specific impedances (ASI) vs. Li content in the $LiNi_{0.5-x}Co_{2x}Mn_{1.5-x}O_4$ ($0 \le 2x \le 0.2$).

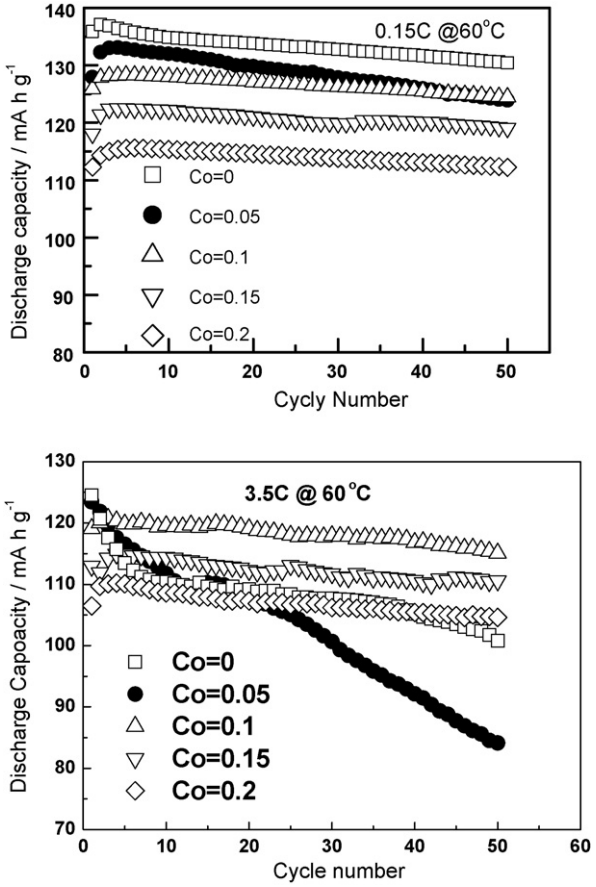

Fig. 9. Cyclic performance of the $LiNi_{0.5-x}Co_{2x}Mn_{1.5-x}O_4$ ($0 \le 2x \le 0.2$) operated in the voltage range of 3–4.9 V at different C rates at 60 °C.

are 130, 123, 124, 119 and 112 mA h g^{-1} for the samples with $2x = 0$, 0.05, 0.1, 0.15 and 0.2, respectively. The capacity losses are 7, 11, 3, 3, and 3 mA h g^{-1} for the samples with $2x = 0$, 0.05, 0.1, 0.15 and 0.2, respectively. When cells were cycled at 3.5 C, both $LiNi_{0.5}Mn_{1.5}O_4$ and $LiNi_{0.475}Co_{0.05}Mn_{1.475}O_4$ exhibited a reduced cyclic performance, while samples with $2x \geq 0.1$ showed an excellent cyclic performance even they were operated at a high rate and at elevated temperature. In our previous study, we reported that the cycleability degradation of the $LiNi_{0.5}Mn_{1.5}O_4$ should be related to the kinetic factors [15], thus we believed that the excellent cyclic performance of the samples with $2x \geq 0.1$ should mainly originate from the increase in the lithium diffusion coefficient as well as the decrease in the area specific impedance.

4. Conclusion

The substitution of cobalt for Ni and Mn in the $LiNi_{0.5}Mn_{1.5}O_4$ resulted in significant structural and electrochemical variations, such as the change in the structural transformation with lithium extraction, the increase in the lithium diffusion coefficient and the decrease in the area specific impedance. The improved kinetic properties caused by the Co substitution for Ni and Mn resulted in the improved electrochemical performances when they were operated at a high rate and at elevated temperature.

Acknowledgement

This work was financially supported by the Scientific Frontier Project from the Ministry of Education, Science, Sports and Culture, Japan.

References

[1] K. Amine, H. Tukamoto, H. Yasuda, Y. Fujita, J. Electrochem. Soc. 143 (1996) 1607.
[2] Q. Zhong, A. Bonakdarpour, M. Zhang, Y. Gao, J. Dahn, J. Electrochem. Soc. 144 (1997) 205.
[3] Y. Gao, K. Myrtle, M. Zhang, J.N. Reimer, J.R. Dahn, Phys. Rev. B 54 (1996) 16670.
[4] T. Zheng, J.R. Dahn, Phys. Rev. B 56 (1997) 3801.
[5] T. Ohzuku, S. Takeda, M. Iwanaga, J. Power Sources 81–82 (1999) 90.
[6] T. Ohzuku, K. Ariyoshi, S. Yamamoto, Y. Makimura, Chem. Lett. (2001) 1270.
[7] Y. Terada, K. Yasaka, F. Nishikawa, T. Konishi, M. Yoshio, I. Nakai, J. Solid State Chem. 156 (2001) 286.
[8] R. Alcándara, M. Jaraba, P. Lavera, J. Tirado, Electrochim. Acta 47 (2002) (1829).
[9] Y.S. Lee, Y.K. Sun, S. Ota, T. Miyashita, M. Yoshio, Electrochem. Commun. 4 (2002) 989.
[10] S.T. Myung, S. Komaba, N. Kumakai, H. Yashiro, H.T. Chung, T.H. Cho, Electrochim. Acta 47 (2002) 2543.
[11] T. Ohzuku, K. Ariyoshi, S. Yamamoto, J. Ceram. Soc. Jpn. 110 (2002) 501.
[12] K. Dokko, M. Mohamedi, N. Anzue, T. Itoh, I. Uchida, J. Mater. Chem. 12 (2002) 3688.
[13] Y. Idemoto, H. Narai, N. Koura, J. Power Sources 119–121 (2003) 125.
[14] J.H. Kim, S.T. Myung, C.S. Yoon, S.G. Kang, Y.K. Sun, Chem. Mater. 16 (2004) 906.
[15] D. Li, Atsushi Ito, K. Kobayakawa, H. Noguchi, Yuichi Sato, Electrochim. Acta 52 (2007) 1919.
[16] J.H. Kim, C.S. Yoon, S.T. Myung, J. Prakashi, Y.K. Sun, Electrochem. Solid-State Lett. 7 (2004) A216.
[17] K. Ariyoshi, Y. Iwakoshi, N. Nakayama, T. Ohzuku, J. Electrochem. Soc. 151 (2004) A296.
[18] Y. Idemoto, H. Sekine, K. Ui, N. Koura, Solid State Ionics 176 (2005) 299.
[19] Y. Ein-Eli, J.T. Vaughey, M.M. Thackeray, S. Mukerjee, X.Q. Yang, J. McBreen, J. Electrochem. Soc. 146 (1999) 908.
[20] G.T.K. Fey, C.Z. Lu, T.P. Kumar, J. Power Sources 115 (2003) 332.
[21] R. Alcántara, M. Jaraba, P. Lavela, J.L. Tirado, E. Zhecheva, R. Stoyanova, Chem. Mater. 16 (2004) 1573.
[22] R. Alcántara, M. Jaraba, P. Lavela, J.L. Tirado, J. Electrochem. Soc. 151 (2004) A53.
[23] D. Li, Atsushi Ito, K. Kobayakawa, H. Noguchi, Yuichi Sato, J. Power Sources 161 (2006) 1241.
[24] J. Kim, S. Myung, C. Yoon, I. Oh, Y. Sun, J. Electrochem. Soc. 151 (2004) A1191.